The relative contribution of fast and slow sinking particles to ocean carbon export

J. Riley, R. Sanders, C. Marsay, F. Le Moigne, E. P Achterberg, A. Poulton

The relative contribution of fast and slow sinking particles to ocean carbon export

J. S. Riley,[1] R. Sanders,[2] C. Marsay,[1,2] F. A. C. Le Moigne,[2] E. P. Achterberg,[1] and A. J. Poulton[2]

Received 25 March 2011; revised 29 September 2011; accepted 27 January 2012; published 20 March 2012.

[1] Particulate organic carbon (POC) generated by primary production and exported to depth, is an important pathway for carbon transfer to the abyss, where it is stored over climatically significant timescales. These processes constitute the biological carbon pump. A spectrum of particulate sinking velocities exists throughout the water column, however numerical models often simplify this spectrum into suspended, fast and slow sinking particles. Observational studies suggest the spectrum of sinking speeds in the ocean is strongly bimodal with >85% POC flux contained within two pools with sinking speeds of <10 m day^{-1} and >350 m day^{-1}. We deployed a Marine Snow Catcher (MSC) to estimate the magnitudes of the suspended, fast and slow sinking pools and their fluxes at the Porcupine Abyssal Plain site (48°N, 16.5°W) in summer 2009. The POC concentrations and fluxes determined were 0.2 μg C L^{-1} and 54 mg C m^{-2} day^{-1} for fast sinking particles, 5 μg C L^{-1} and 92 mg C m^{-2} day^{-1} for slow sinking particles and 97 μg C L^{-1} for suspended particles. Our flux estimates were comparable with radiochemical tracer methods and neutrally buoyant sediment traps. Our observations imply: (1) biomineralising protists, on occasion, act as nucleation points for aggregate formation and accelerate particle sinking; (2) fast sinking particles alone were sufficient to explain the abyssal POC flux; and (3) there is no evidence for ballasting of the slow sinking flux and the slow sinking particles were probably entirely remineralised in the twilight zone.

Citation: Riley, J. S., R. Sanders, C. Marsay, F. A. C. Le Moigne, E. P. Achterberg, and A. J. Poulton (2012), The relative contribution of fast and slow sinking particles to ocean carbon export, *Global Biogeochem. Cycles*, *26*, GB1026, doi:10.1029/2011GB004085.

1. Introduction

[2] The transfer of particulate organic carbon (POC) from the surface ocean to depth, is termed the biological carbon pump [*Boyd and Trull*, 2007] and has the capacity to modify atmospheric carbon dioxide concentrations over climatically significant timescales [*Sigman and Boyle*, 2000]. As POC sinks through the twilight zone (ranging from the base of the euphotic zone to ~1000 m depth [*Buesseler and Boyd*, 2009]) up to 90% may be remineralised [*Martin et al.*, 1987] into inorganic forms by heterotrophic activity and returned to the surface ocean through vertical mixing [*Robinson et al.*, 2010]. Sequestration only occurs when POC sinks below the maximum depth of the winter mixed layer (~1000 m) and into the deep ocean [*Buesseler et al.*, 2007b]. However, the efficiency of oceanic POC sequestration (elaborated upon by *Boyd and Trull* [2007]) is low with only ~1% of total primary production reaching abyssal depths of 3000 m [*Poulton et al.*, 2006].

[3] Two types of sinking particle are considered to be the main vectors of POC export; faecal pellets and aggregates (also called marine snow). Faecal pellets, formed by zooplankton, have high densities and enhanced sinking speeds [*Wilson et al.*, 2008] which range between 5–2700 m day^{-1} depending on the species of origin [*Turner*, 2002]. Marine snow is broadly defined as aggregates >500 μm [*Alldredge and Silver*, 1988] with sinking rates between 10 and 386 m day^{-1} [*Alldredge and Gotschalk*, 1988; *Nowald et al.*, 2009]. The density and composition of individual aggregates is dependent upon the local plankton community structure [*Alldredge and Gotschalk*, 1990].

[4] Ballasting of POC with biominerals is thought to facilitate its transfer to the deep ocean. However, the mechanism driving the relationship between POC and biominerals is uncertain [*De La Rocha and Passow*, 2007]. Biomineral or lithogenic ballasting of sinking POC potentially protects the sinking POC from mesopelagic remineralisation [*Francois et al.*, 2001; *Armstrong et al.*, 2002]. Furthermore, the entrainment of extra density into sinking POC via the incorporation of biominerals and lithogenic material

[1]School of Ocean and Earth Science, National Oceanography Centre Southampton, University of Southampton, Southampton, UK.
[2]National Oceanography Centre Southampton, Southampton, UK.

0886-6236/12/2011GB004085

facilitates POC transfer between the euphotic zone and the deep (>1000 m) ocean [*Klaas and Archer*, 2002; *Sanders et al.*, 2010]. Alternatively, POC may act as a glue, sticking biominerals together which would otherwise have been too small to sink [*Passow*, 2004; *Passow and De La Rocha*, 2006]. Within the scope of this paper we use the term ballast to discuss the addition of density into sinking POC via heavy biomineral fractions.

[5] Direct observations of bulk POC fluxes can be made using a range of instrumentation. The deployment of tethered sediment traps is restricted to the deep (>3000 m) ocean due to under-trapping effects in the upper ocean [*Buesseler et al.*, 2007a]. Tethered Indented Rotating Sphere Carousels (IRSC) sediment traps, which collect data in both a traditional sediment trap and more novel settling velocity modes [*Peterson et al.*, 1993, 2005] and free drifting sediment traps, including PELAGRA (Particle Export measurement using a LAGRAngian trap [*Lampitt et al.*, 2008]) and NBSTs (Neutrally Buoyant Sediment Traps [*Buesseler et al.*, 2000]) minimize POC under-trapping effects and are deployed in the upper ocean. Radiochemical tracer techniques such as thorium-234 (^{234}Th) can also be used to estimate POC fluxes throughout the water column [*Buesseler et al.*, 1993; *van der Loeff et al.*, 2006]. Individual particles can be collected throughout the water column using technologies such as Marine Snow Catchers [*Lampitt et al.*, 1993] and polyacrylamide gels [*Lundsgaard*, 1995; *Ebersbach and Trull*, 2008].

[6] When considering carbon export from a biogeochemical perspective POC is often grouped (by sinking speed) into three pools, consisting of a small proportion of fast sinking particles, a second class of slower sinking particles and a remaining suspended particle field, despite this being an oversimplification of a complex spectra of particle sinking speeds [*Fasham et al.*, 1990; *Kriest and Evans*, 1999; *Boyd and Stevens*, 2002]. Direct observations of the spectra of particle sinking speeds, compiled from a global data set using an IRSC suggest that slow sinking particles (sinking speeds ranging between 0.7–11 m day^{-1}), account for ~60% of the total POC flux while sinking speeds >326 m day^{-1} contribute ~25% to the total POC flux. Overall >85% of the global carbon flux can be explained by a strongly bimodal distribution of sinking speeds although some geographical variability is apparent [*Alonso-González et al.*, 2010].

[7] In this study we present observational POC standing stock and flux data, collected using a Marine Snow Catcher (MSC). The MSC is a large volume (100 L) water bottle (Figure 1) consisting of two detachable sections. Upon deployment in the water column the MSC is closed at depth using a messenger operated closure release. Water enters the bottle during descent through the water column via two large terminal openings, designed to minimize turbulent flow of water into the bottle. Post deployment the MSC is placed on deck for 2 h while any particles present settle onto the base of the bottom 7 L chamber. After settling, the top 93 L of water is drained off gently to avoid mixing of water in the top and base sections. During this draining process no physical separation of the top and base water samples occurs. The upper section of the MSC is then detached, leaving any particles on the bottom of the 7 L base section.

[8] This study presents upper ocean POC, calcite and opal standing stock and flux data for three pools, suspended, fast sinking and slow sinking which have been operationally defined by the 2 h settling period. The suspended pool consists of those particles which remain in the upper section of the MSC following settling and have no flux. Fast sinking material is defined as aggregated particles picked off the bottom of the base chamber, while the slow sinking pool is determined from the difference in particle concentrations between the top and base sections of the MSC. We validate our calculations with contemporaneous measurements of POC fluxes and go on to discuss the potential formation mechanisms of fast sinking particles and the transfer and ballasting of POC fluxes into the deep ocean.

2. Methods

2.1. Site Description

[9] Sinking particles were collected at the Porcupine Abyssal Plain (PAP) site (48°N, 16.5°W) using the MSC during RRS *Discovery* cruise D341 (8th July to 13th August, 2009). The depth of the winter mixed layer at this site is typically ~350 m [*Steinhoff et al.*, 2010] and the annually integrated primary productivity ~200 g C m^{-2} y^{-1} [*Lampitt et al.*, 2010].

2.2. Particle Collection

[10] The MSC was deployed nine times (see Table S1 of the auxiliary material for precise locations) at 50 m depth, which corresponded to the approximate depth of the mixed layer at the time of sampling.[1] In total, 459 individual aggregates which had settled onto the bottom of the base chamber during each settling period, were picked using a Pasteur pipette and classified under an optical microscope. Two categories of particles containing organic matter were observed (Figure 2); Marine Snow Aggregates (MSA, 429 particles) and particles consisting of a distinct solid biomineralising protist center enveloped in marine snow, which we term as Aggregate Protist Complexes (APC, 30 particles). Post settling (2 h) water samples for POC, calcite and opal analysis were collected from the top 93 L and the bottom 7 L chamber of the MSC. Samples of POC, calcite and opal from the top and base sections of the MSC were only available for the last 5 stations. Thus the sinking speed, aggregate area, aggregate POC content, stocks and fluxes presented in this manuscript only corresponds to the last 5 stations. However, when discussing the relative abundance of MSA and APC particles, data from all 9 stations will be used.

2.3. Particle Settling Experiments

[11] The sinking rates of 110 picked particles were determined by placing them in a glass 2 L measuring cylinder, filled with surface seawater from the ship's underway supply and kept at ambient water temperature (~15°C). Individual particles were placed into the measuring cylinder using a Pasteur pipette, a few centimeters below the water surface so any motion was due to natural sinking [*Martin et al.*, 2010].

[1] Auxiliary materials are available in the HTML. doi:10.1029/2011GB004085.

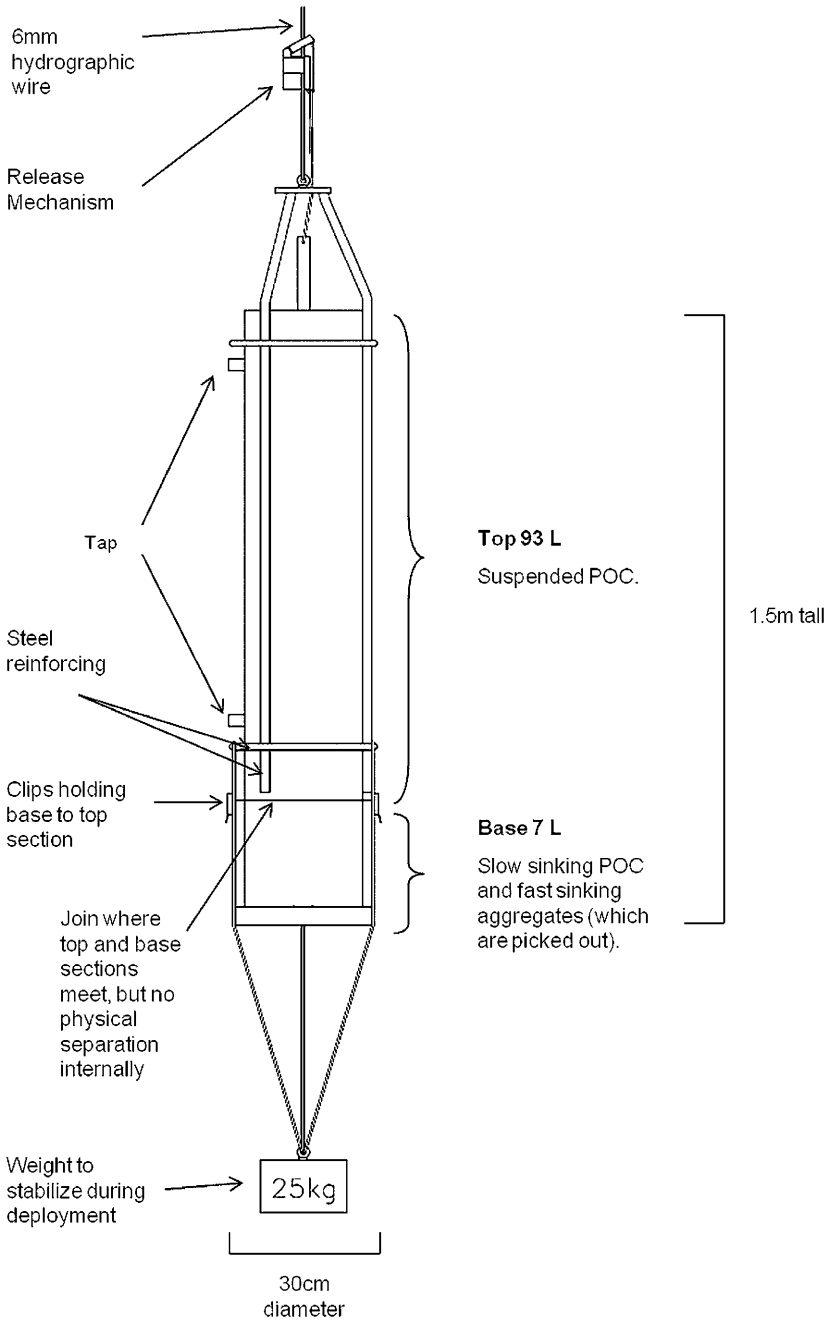

Figure 1. General arrangement of the Marine Snow Catcher.

Two sinking times were recorded as individual particles passed two discrete points within the measuring cylinder. The two sinking rate observations of individual particles from each experiment were highly reproducible, with average standard errors of ±4% for MSA and ±19% for APC.

[12] Particles were retrieved after each experiment using a Pasteur pipette and initial photography of each particle was undertaken on the ship to aid further classification. Particles were then preserved in 5% buffered formalin. High quality images (×4 magnification) of the preserved particles were taken after the cruise, using a camera microscope (Meiji Techno Japan MX microscope with an Infinity 1 camera).

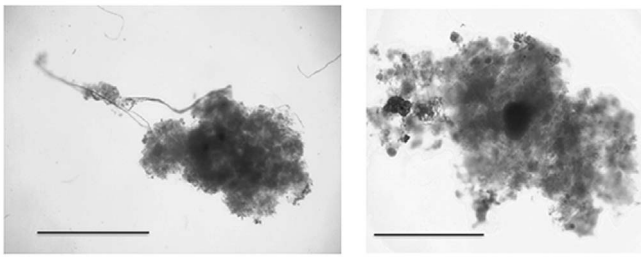

Marine Snow Aggregate Aggregate – protist complex

Figure 2. Examples of the types of particle identified. The scale bar in each is 1 mm.

Table 1. Suspended, Fast Sinking and Slow Sinking POC and Opal Concentrations, Calculated After 2 h Settling Period

Station Number	Fast Sinking POC Concentration (μg L^{-1})	Slow Sinking POC Concentration (μg L^{-1})	Suspended POC Concentration (μg L^{-1})	Total POC Concentration (μg L^{-1})	Suspended Opal Concentration (μg L^{-1})	Slow Sinking Opal Concentration (μg L^{-1})
16589	0.2	5	109	115	5	0.1
16593	0.1	6	119	125	3	0.5
16605	0.1	4	78	82	No Data	No Data
16620	0.2	5	89	94	4	0.4
16660	0.3	5	92	97	2	0.3
Average	0.2	5	97	103	3	0.3
SD	0.1	1	17	10	1	0.2
Av (%)	0.2	5	95	100	-	-
RSD[a] (%)	47	12	17	9	-	-

[a]RSD is the relative standard deviation, expressed as a percentage.

Comparison of photographs for 11 particles taken at sea and post cruise constrained changes in particle area due to storage and preservation at ± 17%.

2.4. POC, Calcite and Opal Determination

[13] Concentrations of POC in the top and the base of the MSC were determined by filtration of 1.5–2 L of water onto pre-combusted (450°C, 12 h) glass fibre filters (25 mm diameter GF/F, Whatman). Filters were stored in petri dishes at −20°C, acid fumed and analyzed using an elemental analyzer (Thermo Finnegan Flash EA1112). The concentration of POC contained within the total aggregates collected from each deployment was calculated using the empirical relationship proposed by *Alldredge* [1998]. Calcite measurements were made on 1–1.5 L water samples from the top and base of the MSC, filtered onto 0.8 μm polycarbonate membrane filters (Whatman). Samples were rinsed with a slightly alkaline (pH 9) de-ionised water rinse solution to remove any remaining seawater and frozen at −20°C prior to analysis. In the laboratory samples were extracted in 2% nitric acid and analyzed using Inductively Coupled Plasma Optical Emission Spectrometry (Perkin Elmer Optima 4300 DV ICP-OES). For opal determination 1–1.5 L of seawater was filtered onto 0.8 μm polycarbonate filters (Whatman), digested using 0.2 M sodium hydroxide (80°C, 4 h) and then neutralised with 0.1 M hydrochloric acid. Silicate concentrations were subsequently determined using a auto-analyser (Skalar Sanplus) [*Poulton et al.*, 2006].

2.5. Calculation of the Slow and Fast Sinking Particle Concentrations

[14] Assuming the base concentration is greater than the top concentration after the to hour settling period the slow sinking particle concentrations were determined. The difference in concentration in the top and base of the MSC enables the excess of carbon in the base (7 L) of the MSC to be calculated. This difference must then be scaled to the ratio of the base: total volume of the MSC:

$$\text{Slow Sinking Concentration}\left(\mu\text{g L}^{-1}\right) = \left(\text{Conc.}_{\text{Base}} - \text{Conc.}_{\text{Top}}\right) \times R_{B:T} \quad (1)$$

where $\text{Conc.}_{\text{Base}}$ and $\text{Conc.}_{\text{Top}}$ are the concentrations in the base and top sections of the MSC respectively and $R_{B:T}$ is the ratio of the base volume (7 L) to the total volume (100 L) i.e., $\frac{7}{100}$ or 0.07.

[15] Fast sinking POC concentrations were determined by calculating the total mass of POC carried in the fast sinking aggregates as a fraction of the total volume of the MSC:

$$\text{Fast Sinking POC}\left(\mu\text{g L}^{-1}\right) = {POC_{Agg} \times N}\Big/{V_{Total}} \quad (2)$$

where POC_{Agg} is the average mass of POC per aggregate calculated following *Alldredge* [1998], N is the total number of aggregates collected during each deployment and V_{Total} is the total volume of the MSC (100 L; Figure 1). This equation cannot be applied to calculate the fast sinking opal or calcite concentrations since no literature conversion factor is available. Thus estimates for calcite and opal were not calculated.

2.6. Calculation of Fluxes

[16] Fluxes were calculated following standard calculations dividing mass by area and time. However, given the base volume of 7 L, a top volume of 93 L and an assumption of a homogenous distribution of particles throughout the entire MSC at the start of the settling period, 7% of the sinking material must have originated in the base section. Therefore we scale our final flux value to 93% to account for this:

$$\text{Flux}\left(\mu\text{g m}^{-2}\text{day}^{-1}\right) = \left({{Mass}\Big/{MSC\ Area}}\Big/{Sinking\ Time}\right) \times F_{Top} \quad (3)$$

where the term *Mass* applies to the mass of slow or fast sinking particles indentified in the MSC, the *MSC Area* is the horizontal footprint of the base chamber (0.06 m^2; Figure 1), the *Sinking Time* is the time taken for either the fast or slow particles to sink (see section 3.3) and F_{Top} is the fraction of POC not in the base section at the start of the settling period (i.e., 93 L out of 100 L or 0.93). The total flux was calculated from the sum of the slow and fast fluxes.

3. Results

3.1. POC, Calcite and Opal Concentrations in the Top and Base Chambers of the MSC

[17] The average concentration of POC (±1 standard deviation [S.D.]) in the water from the top section of the MSC across all stations sampled after the 2 h settling was 97 (±17) μg C L^{-1} while the average concentration of POC in the water from the bottom chamber was 170 (±24) μg C L^{-1}. The average concentrations in the top and base of the MSC

Table 2. Data for Calculation of, Aggregate POC Content, Total Mass of Fast Sinking POC and Fast Sinking Concentration for Each MSC Deployment

Station Number	N[a]	Average ESV[b] (mm^{-3})	Average POC[c] ($\mu g\ agg^{-1}$)	Total Mass[d] (μg C)	Total Concentration[e] ($\mu g\ C\ L^{-1}$)
16589	30	0.4 (±0.3)	0.6 (±0.1)	19 (±3)	0.2 (±0.03)
16593	17	0.2 (±0.2)	0.5 (±0.1)	8 (±1)	0.1 (±0.01)
16605	19	0.2 (±0.3)	0.5 (±0.1)	9 (±1)	0.1 (±0.01)
16620	30	0.5 (±0.6)	0.7 (±0.1)	21 (±3)	0.2 (±0.03)
16660	53	0.3 (±0.2)	0.5 (±0.1)	26 (±4)	0.3 (±0.04)
Average		0.3	0.6	17	0.2
SD		0.1	0.1	8	0.1

[a]The total number of MSA and APC picked from the base of the MSC in 100 L.

[b]Particle areas were measured using the image analysis software Image-J [*Abramoff et al.*, 2004], calibrated using a stage graticule under magnification identical to the particle. From this average particle ESV was calculated per station with associated standard deviation (shown in brackets).

[c]Calculated using the average ESV and the empirical relationship proposed by *Alldredge* [1998]; POC ($\mu g\ agg^{-1}$) = 0.99 × ESV (mm^{-3})$^{0.52}$. The values in the brackets represent the maximum and minimum range of possible concentrations for the particle carbon content, given the quoted standard errors in the work of *Alldredge* [1998].

[d]The total mass of fast sinking POC is calculated by from the average POC content per aggregate at each station by the number of aggregates collected at each station (equation (2)).

[e]The total concentration of fast sinking POC is then calculated by dividing the total mass by the volume of the MSC (100 L; equation (2)).

were normally distributed and the differences between the top and base were significantly different from one another (Student t-test, $p < 0.001$), consistent with a slow sinking flux of POC occurring within the MSC during the settling period.

[18] The average concentrations of calcite in the top and base water samples from the MSC were 4 (±3) $\mu g\ L^{-1}$ and 8 (±3) $\mu g\ L^{-1}$, respectively. Statistical analysis showed a normal distribution of concentrations however a Student t-test indicates that the mean top and base values were not significantly different ($p < 0.1$). Further analysis using Pearson's correlation coefficient also showed no significant relationship ($p < 0.37$) between the top and base concentrations. This suggests either that there was little or no slow sinking flux of calcite within the MSC during the settling period or that the distribution of calcite was patchy across the sampling site and more extensive sampling was needed to identify any relationship.

[19] The average concentrations of opal within the top and base of the MSC were 3 (±1) $\mu g\ L^{-1}$ and 8 (±2) $\mu g\ L^{-1}$ respectively. The range of concentrations was not normally distributed and results of a Mann Whitney-U test indicated a significant difference ($p < 0.03$) between the top and bottom chambers. This implies that there was a flux of opal into the base of the MSC during the settling period. (See Tables S2, S3 and S4 of the auxiliary material for POC, calcite and opal concentrations measured at each station.)

3.2. POC and Opal Concentration of Suspended, Slow and Fast Sinking Pools

[20] Suspended concentrations were assumed to be the material remaining in the top section of the MSC after the 2 h settling period, slow sinking concentrations were calculated following equation (1) (see Table 1 and Tables S4 and S5 of the auxiliary material) and fast sinking concentrations were calculated following equation (2) (see Table 2). We are confident we have measured the total pool of POC present within the MSC since all of the fast sinking particles were picked and the total concentration of the slow sinking particles was measured by homogenising the remaining 7 L in the base chamber (after removal of the fast sinking aggregates) prior to filtering a 2 L sub sample.

[21] Concentrations of POC averaged across all stations (±1 S.D.) within the fast sinking, slow sinking and suspended fractions were 0.2 (±0.1), 5 (±1) and 97 (±17) $\mu g\ C\ L^{-1}$ respectively (Table 1). Fast sinking POC contributed (with relative standard deviations) 0.2 (±47) % while the slow sinking fraction and suspended material contributed ~5 (±12) % ~95 (±17) % in terms of total POC (Figure 3). The mean suspended concentration of opal within the MSC was 3 (±1) $\mu g\ L^{-1}$ while the mean slow sinking pool was 0.3 (±0.2) $\mu g\ L^{-1}$ (Table 1; see auxiliary material for full data tables documenting the calculation of the slow sinking pools of POC and opal). No data for opal content of the fast sinking aggregated particles were available. Furthermore, no concentrations of calcite were calculated for the three pools since there was no significant difference between the average top and base sections concentrations of the MSC (section 3.1). Unfortunately the lack of opal and calcite data for the fast sinking pool prevents us from investigating how the fast and slow sinking biomineral pools scale relatively to each other.

3.3. Sinking Speeds of Slow and Fast Pools

[22] The sinking speed of the slow settling fraction was estimated assuming; first that all of the fast sinking MSA particles had been picked from the base chamber, ensuring the fast and slow particle pools are separated from one another; and second that the slow sinking particles were homogenously distributed within the MSC prior to settling. The sinking speed of particles can be calculated following equation (4). The sinking time was constant at 2 h (0.083 days), thus the only variable is the distance the particles sank, assuming that all of the slow sinking particles had reached the base section. Assuming a homogenous distribution of particles at the start of the 2 h settling period, particles are estimated to sink at an average of 9 m day^{-1}settling from the midpoint of the MSC (0.75 m) but may range between ~0 m day^{-1} and 18 m day^{-1} depending on the starting location of a slow sinking particle in the MSC.

[23] The sinking speed of the fast pool was determined as a weighted average (±1 S.D.) of the MSA (average of 180 (±22) m day^{-1}) and the APC (average of 232 (±58) m day^{-1}) settling speeds determined in the

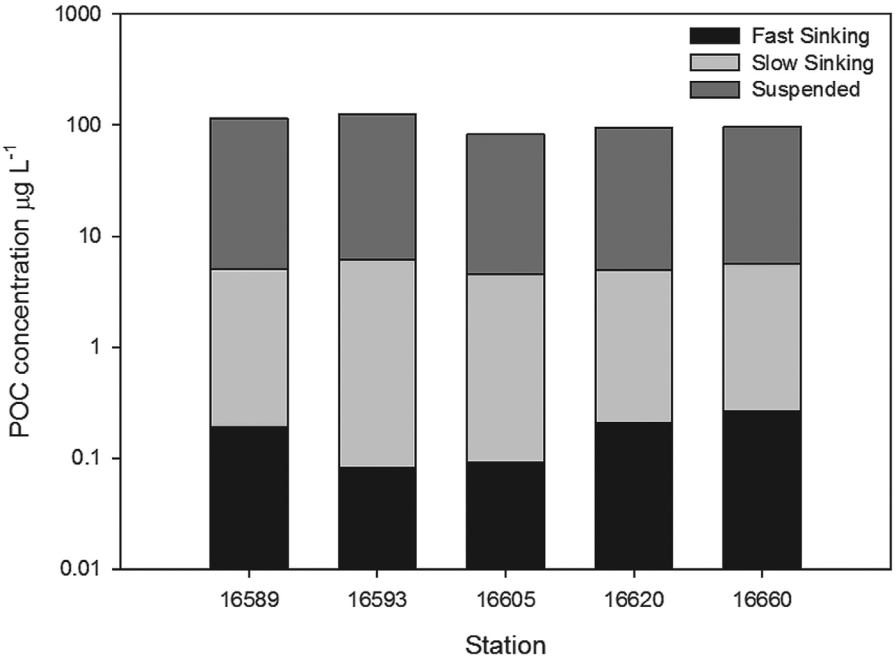

Figure 3. POC concentrations of the suspended, slow and fast sinking pools (note the logarithmic scale on the *y* axis).

sinking experiments. Overall, the weighted average sinking speed of the fast sinking pool is 181 ± 8 m day^{-1}, with a sinking time of ~0.005 days.

$$\text{Sinking Speed}\left(\text{m day}^{-1}\right) = {}^{\text{Distance}}/_{\text{Time}}. \quad (4)$$

3.4. Export Fluxes of POC and Opal

[24] The average (±1 S.D.) fast sinking POC flux across all stations was calculated to be 54 (±25) mg C m^{-2} day^{-1} (~37 (±47) % of the total flux) while the average slow sinking POC flux, was 92 (±11) mg C m^{-2} day^{-1} (~63 (±12) % of the total flux; Table 3). Overall we determine a total flux of POC at the base of the mixed layer (both fast and slow sinking pools) of 146 (±26) mg C m^{-2} day^{-1}. An opal export flux of 6 (±3) mg C m^{-2} day^{-1} (Table 3) was calculated for the slow sinking fraction, no calculation could be made for the fast or total fluxes since no data were available for the fast sinking particle opal content.

4. Discussion

4.1. Comparison of MSC POC Fluxes With Other Upper Ocean Flux Estimates

[25] The averaged total POC fluxes at the PAP site for the period 2003–2005, obtained from PELAGRA deployments, were 72 mg C m^{-2} day^{-1} in the upper 175 m of the water column (Figure 4) [*Lampitt et al.*, 2008]. A PELAGRA deployment (4th–6th August, cruise D341), concurrent with the MSC deployments presented in this paper, determined a POC flux of 84 (±8) mg C m^{-2} day^{-1} at 51 m, which was close to the total POC flux determined using the MSC (146 (±26) mg C m^{-2} day^{-1}, Figure 4). The broad similarity of flux measurements between PELAGRA and MSC

Table 3. Calculated Masses and Fluxes of POC and Opal After the 2 h Settling Period[a]

Station Number	Mass of Fast Sinking POC (μg)	Mass of Slow Sinking POC (μg)	Flux of Fast Sinking POC (mg m^{-2} d^{-1})	Flux of Slow Sinking POC (mg m^{-2} d^{-1})	Mass of Slow Sinking Opal (μg)	Flux of Slow Sinking Opal (mg m^{-2} d^{-1})
16589	19	488	61	88	13	2
16593	8	602	26	109	51	9
16605	9	444	30	80	No Data	No Data
16620	21	470	67	85	41	8
16660	26	535	85	97	32	6
Average	17	508	54	92	34	6
SD	8	62	25	11	16	3
Av (%)	-	-	37	63	-	-
RSD (%)	-	-	47	12	-	-

[a]See Tables S5 and S6 of the auxiliary material, for further details about the calculation of mass. Fluxes following equation (3)).

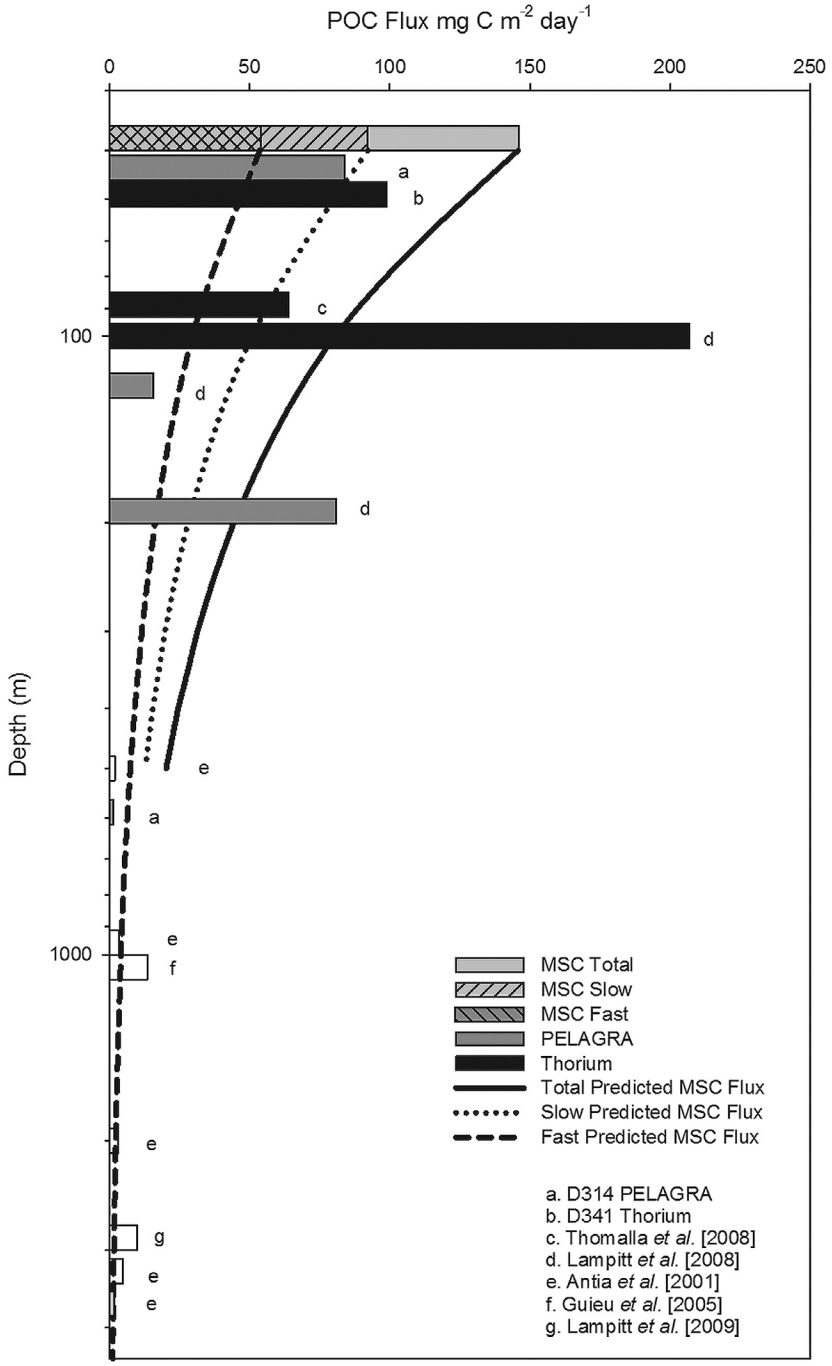

Figure 4. Comparison of C flux estimates using different sampling techniques with MSC data. Superimposed on top of this is the predicted POC flux values from the MSC based on the *Martin et al.* [1987] equation.

suggests the MSC is capable of producing comparable estimates of upper ocean POC fluxes.

[26] An alternative approach used to estimate POC export uses the particle reactive tracer ^{234}Th [*Buesseler et al.*, 1993; *van der Loeff et al.*, 2006]. Export measurements in the vicinity of the PAP site have been made on a number of occasions since 1993 using the ^{234}Th technique (Figure 4). *Thomalla et al.* [2008] determined a POC flux of 64 mg C m^{-2} day^{-1} at 100 m and *Lampitt et al.* [2008] estimated a flux of 207 mg C m^{-2} day^{-1} at 100 m. Measurements of ^{234}Th made at the PAP site during cruise D341 yielded a station average flux of 99 ($\pm$41) mg C m^{-2} day^{-1} at 56 m (Figure 4). It is clear that there is variability in the estimates of C flux made using the ^{234}Th technique, however the contemporaneous data is comparable with the flux estimates made using the MSC (146 mg C m^{-2} day^{-1}).

4.2. Assessment of the Validity of the Calculations

[27] The calculation of the suspended and slow sinking pools of both POC and opal rely upon the assumption that all

particles within the MSC were homogenously distributed at the beginning of the two hour settling period. Therefore, on average, a slow sinking particle will sink half the height of the MSC (0.75 m) in two hours and have an average settling velocity of 9 m $day^{-1.}$ However, some particles will clearly settle faster or slower than this, resulting in an under or over estimation of the sinking speed. An increase in the sinking velocity of the slow sinking fraction, greater than 9 m day^{-1}, as assumed in section 3.3, would result in an even larger flux than that estimated from the ^{234}Th or PELAGRA, hence we consider this scenario unlikely given the MSC flux is higher than either the PELAGRA or the ^{234}Th derived flux.

[28] Conversely, some particles will originate above the midpoint of the MSC and not penetrate the base section during the 2 h settling period, leading to a potential underestimation of the slow sinking pool and an overestimation of the suspended pool. We estimate the potential impact of such a scenario by deriving two simultaneous equations, to calculate the suspended and slow sinking POC, assuming 50% of the slow sinking flux had not penetrated the base section. Under this revised estimate the general distribution of material in the various classes is similar to that found under our initial assumptions, with POC concentrations in the suspended, slow and fast sinking pools being 89%, 10% and <1% respectively (see Table S7 and Text S1 of the auxiliary material).

[29] Using this new slow sinking pool size to estimate the associated flux (assuming a sinking speed of 9 m day^{-1} and that particles sank from the midpoint of the MSC in 2 h), gives a slow sinking flux of 191 mg C m^{-2} day^{-1}. When added to the fast POC flux a total flux estimate of 245 mg C m^{-2} day^{-1} was calculated. This total MSC POC flux is approximately 40% greater than our initial estimate (146 mg C m^{-2} day^{-1}) and approximately 60% greater than independent estimates made using PELAGRA (84 mg C m^{-2} day^{-1}) and ^{234}Th (99 mg C m^{-2} day^{-1}). It therefore seems likely that our initial estimate of the size of the slow sinking pool was relatively robust and that the range of sinking speeds between ~0 and 18 m day^{-1} with an average of ~9 m day^{-1} is also reasonably close to reality.

4.3. Formation of Fast Sinking Particles

[30] *Lee et al.* [2009] suggest a 'catalyst' initiates the aggregation process which forms fast sinking particles. An increase in bulked POC flux observed at the PAP site during 2001 correlated with observed increases in radiolarian populations [*Lampitt et al.*, 2009], which may have acted as a nucleation point promoting fast sinking particle aggregation. Of the fast sinking particles identified across all 9 deployments 30 consisted of organic matter aggregated around a biomineralised protist (APC, Figure 2). This suggests that the presence of planktonic organisms can indeed act as nucleation points for individual particle aggregation and accelerate their sinking rate. However, since APC contributed such a small proportion of total sinking material collected, other 'catalysts' must also be important. These may include the production of sticky transparent exopolymer particles (TEP) [*Alldredge and Gotschalk*, 1990; *Passow et al.*, 2001] by diatoms.

4.4. Fluxes of POC to the Deep Ocean

[31] Large (>53 μm) rapidly sinking particles are thought to be relatively rare within the water column [*McCave*, 1975], with estimates of fast sinking particle concentrations in the Indian Ocean and Panama Basin contributing 3–15% to total POC [*Mullin*, 1965; *Bishop et al.*, 1980]. *Alonso-González et al.* [2010] suggest fast sinking particles alone supply the abyssal POC flux due to their rapid transit time through the water column. The fast sinking particles collected in this study, with an equivalent spherical diameter of 195–1639 μm, contributed 0.2 (±47) % to the total POC concentration (Figure 3). However, given the small contribution of fast sinking particles and the remineralisation processes which occur within the twilight zone it is unclear whether these particles would truly sustain the observed POC fluxes to the abyss.

[32] Applying the flux attenuation parameterization of *Martin et al.* [1987] to our fast sinking flux estimates (54 (±25) mg C m^{-2} day^{-1}; section 3.4) we predict a deep flux of 2 mg C m^{-2} day^{-1} (at 3000 m, Figure 4), close to the deep sediment trap flux estimates of 1.8–10 mg C m^{-2} day^{-1} at 3000–3500 m [*Antia et al.*, 2001; *Lampitt et al.*, 2009]. Applying the same *Martin et al.* [1987] parameterization to our 50 m total flux value (146 mg C m^{-2} day^{-1}; the sum of the fast and slow flux values) yields a deep flux estimate of 4 mg C m^{-2} day^{-1}, also within the range of the deep sediment trap fluxes. Thus based on the predicted attenuated flux values we are unable to determine whether fast sinking particles alone or a combination of fast and slow fluxes supply POC to the deep ocean.

[33] Deep sediment trap data indicate a seasonal flux of POC to the seafloor, with peak fluxes lagging the maxima in surface productivity by ~40 days [*Lampitt et al.*, 2010]. The determined sinking speeds of 181 m day^{-1} and 9 m day^{-1} (see section 3.3) for the fast and slow sinking particles results in a transit time between 50 and 4500 m of ~30 and 500 days respectively. The 40 day lag time between primary maxima in primary productivity and deep POC fluxes, and the estimated transit time of the fast sinking flux are comparable, implying fast sinking particles are the major contributor to the deep sediment trap fluxes [*Alonso-González et al.*, 2010] undergoing reduced remineralisation [*Wakeham et al.*, 2009]. The long transit time of the slow sinking POC suggests complete remineralisation in the upper water column. Furthermore, if the slow sinking particles were to reach the abyss, the long transit time to the deep ocean would likely mask any seasonal signal observed in the deep sediment traps. Thus we surmise slower sinking particles are at this site equally important in terms of total flux out of the euphotic zone but contribute negligibly to abyssal carbon transfer.

4.5. Does a Biomineral Ballasting Effect Occur?

[34] We are unable to quantitatively comment upon the relationship between biomineral and POC concentrations of the fast sinking particles due to a lack of data on the calcite and opal contents. Despite this, the APC sank approximately 50% faster (~232 (±58) m day^{-1}) than MSA (~180 (±22) m day^{-1}; section 3.3). This implies that some component of the fast flux is actively ballasted. This is consistent with the observed pulses of POC to the abyss associated with increases in biomineralising organisms at the PAP site [*Lampitt et al.*, 2009]. Whether the remaining MSA flux is ballasted or simply sinks quickly because the aggregates are large enough to overcome the viscous effects

of seawater [*Alldredge and Gotschalk*, 1988] is a question we cannot address and is an area for future investigation.

[35] The average slow sinking POC flux showed no corresponding flux of calcite in the MSC during settling (section 3.1), suggesting no ballasting relationship with calcite. However, if the distribution of calcite is patchy across the PAP site, a ballasting relationship may still exist in discrete areas. In comparison, a slow sinking flux of opal was calculated (section 3.4) but correlation analysis of the slow sinking opal and POC fluxes revealed no significant relationship (Spearman's Rank Correlation Coefficient, $p < 0.75$, 0.05 confidence level), implying the average flux of POC was not ballasted by opal. From the ^{234}Th derived POC and biomineral fluxes presented by *Sanders et al.* [2010], it was concluded that an upper ocean ballasting relationship was likely. Critical re-examination of their findings identifies a small flux of POC occurring with no associated biomineral flux. We hypothesize this small flux of POC represents the slow sinking flux, which may be unballasted by either calcite or opal.

5. Conclusion

[36] Our work contributes to the growing body of evidence that POC in the surface ocean can be best conceptualised using a three pool model; consisting of suspended, slow sinking and fast sinking fractions, despite being an over-simplification of the global variability in particle sinking speeds. The key findings of this study suggest the following:

[37] 1. The MSC provides a comparable alternative to other technologies as a method of measuring POC stocks and fluxes in the upper ocean, enabling both the occurrence and magnitudes of the fast and slow sinking POC fluxes to be examined.

[38] 2. Nucleation around a biomineralising organism may aid particle formation. This supports the argument by *Lampitt et al.* [2009] that biomineralising protist mediated export may be important at the PAP site.

[39] 3. Fast sinking POC, produced in the euphotic zone contributes negligibly to total POC stocks, but is sufficient to supply POC to the abyss. Further to this we suggest it is, at least in part, ballasted by biominerals and is most important in terms of carbon sequestration.

[40] 4. Slow sinking POC is likely to be remineralised in the twilight zone due to its slow transit time though the water column. Furthermore the slow sinking flux may not be ballasted. We therefore suggest the slow sinking particles are an unlikely source of POC to the abyss.

[41] The geographical extent over which this three pool model is valid is uncertain. However, the synthesis of studies from the Mediterranean and subarctic and subtropical Pacific, presented by *Alonso-González et al.* [2010] strongly support the conclusions drawn here. Therefore it seems likely to have a wider significance than simply the North East Atlantic Ocean. A key question for future research is to define the processes which regulate the relative sizes of the fast and slow sinking pools and the magnitudes of their respective fluxes. For example, it may be the case that a constant background flux of slow sinking material occurs with a fast sinking pool superimposed on it by episodic events such as upwelling, storms, eddies or the spring diatom bloom. Potential shifts in the relative magnitudes of the fast and slow sinking pools, favoring the formation of slow sinking POC may result in a change in the partitioning of CO_2 between the atmosphere and ocean. Thus greater quantities of POC would be respired in the upper ocean, with consequences for global climate [*Kwon et al.*, 2009].

[42] **Acknowledgments.** We would like to thank the crew of the RRS *Discovery* for their assistance with the deployment of the technical equipment. Furthermore, we would like to acknowledge Maria Villa (Servicio de Radioisótopos. Centro de Investigación, Tecnología e Innovación, Universidad de Sevilla), who assisted with the ^{234}Th sampling; Charlotte Marcinko and Nina Rothe (National Oceanography Centre, Southampton), who assisted with the settling experiments; and Kevin Saw and Sam Ward, who coordinated the PELAGRA deployments. Finally, we would also like to thank all the people who have taken the time to provide the useful and insightful comments, which have aided the evolution of this paper. The funding for this project was through NERC SOFI doctoral training grant award (NE/F012462/1).

References

Abramoff, M. D., P. J. Magelhaes, and S. J. Ram (2004), Image processing with ImageJ, *Biophotonics Int.*, *11*(7), 36–42.

Alldredge, A. (1998), The carbon, nitrogen and mass content of marine snow as a function of aggregate size, *Deep Sea Res., Part I*, *45*(4–5), 529–541, doi:10.1016/S0967-0637(97)00048-4.

Alldredge, A. L., and C. Gotschalk (1988), The in situ settling behavior of marine snow, *Limnol. Oceanogr.*, *33*(3), 339–351, doi:10.4319/lo.1988.33.3.0339.

Alldredge, A. L., and C. Gotschalk (1990), The relative contribution of marine snow of different origins to biological processes in coastal waters, *Cont. Shelf Res.*, *10*(1), 41–58, doi:10.1016/0278-4343(90)90034-J.

Alldredge, A. L., and M. W. Silver (1988), Characteristics, dynamics and significance of marine snow, *Prog. Oceanogr.*, *20*(1), 41–82, doi:10.1016/0079-6611(88)90053-5.

Alonso-González, I. J., J. Arístegui, C. Lee, A. Sanchez-Vidal, A. Calafat, J. Fabrés, P. Sangrá, P. Masqué, A. Hernández-Guerra, and V. Benítez-Barrios (2010), Role of slowly settling particles in the ocean carbon cycle, *Geophys. Res. Lett.*, *37*, L13608, doi:10.1029/2010GL043827.

Antia, A. N., et al. (2001), Basin-wide particulate carbon flux in the Atlantic Ocean: Regional export patterns and potential for atmospheric CO_2 sequestration, *Global Biogeochem. Cycles*, *15*, 845–862, doi:10.1029/2000GB001376.

Armstrong, A., C. Lee, J. I. Hedges, S. Honjo, and S. G. Wakeham (2002), A new, mechanistic model for organic carbon fluxes in the ocean based on the quantitative association of POC with ballast minerals, *Deep Sea Res., Part II*, *49*(1–3), 219–236, doi:10.1016/S0967-0645(01)00101-1.

Bishop, J. K. B., R. W. Collier, D. R. Kettens, and J. M. Edmond (1980), The chemistry, biology, and vertical flux of particulate matter from the upper 1500 m of the Panama Basin, *Deep Sea Res., Part A*, *27*(8), 615–640, doi:10.1016/0198-0149(80)90077-1.

Boyd, P. W., and C. L. Stevens (2002), Modelling particle transformations and the downward organic carbon flux in the NE Atlantic Ocean, *Prog. Oceanogr.*, *52*(1), 1–29, doi:10.1016/S0079-6611(02)00020-4.

Boyd, P. W., and T. W. Trull (2007), Understanding the export of biogenic particles in oceanic waters: Is there consensus?, *Prog. Oceanogr.*, *72*(4), 276–312, doi:10.1016/j.pocean.2006.10.007.

Buesseler, K. O., and P. W. Boyd (2009), Shedding light on processes that control particle export and flux attenuation in the twilight zone of the open ocean, *Limnol. Oceanogr.*, *54*(4), 1210–1232, doi:10.4319/lo.2009.54.4.1210.

Buesseler, K. O., M. P. Bacon, J. Kirk Cochran, and H. D. Livingston (1993), Carbon and nitrogen export during the JGOFS North Atlantic Bloom experiment estimated from ^{234}Th: ^{238}U disequilibria, *Deep Sea Res., Part A*, *39*(7–8), 1115–1137, doi:10.1016/0198-0149(92)90060-7.

Buesseler, K. O., D. K. Steinberg, A. F. Michaels, R. J. Johnson, J. E. Andrews, J. R. Valdes, and J. F. Price (2000), A comparison of the quantity and composition of material caught in a neutrally buoyant versus surface-tethered sediment trap, *Deep Sea Res., Part I*, *47*(2), 277–294, doi:10.1016/S0967-0637(99)00056-4.

Buesseler, K. O., et al. (2007a), An assessment of the use of sediment traps for estimating upper ocean particle fluxes, *J. Mar. Res.*, *65*, 345–416.

Buesseler, K. O., et al. (2007b), Revisiting carbon flux through the ocean's twilight zone, *Science*, *316*(5824), 567–570, doi:10.1126/science.1137959.

De La Rocha, C. L., and U. Passow (2007), Factors influencing the sinking of POC and the efficiency of the biological carbon pump, *Deep Sea Res., Part II*, *54*(5–7), 639–658, doi:10.1016/j.dsr2.2007.01.004.

Ebersbach, E., and T. Trull (2008), Sinking particle properties from polyacrylamide gels during the KErguelen Ocean and Plateau compared Study (KEOPS): Zooplankton control of carbon export in an area of persistent natural iron inputs in the Southern Ocean, *Limnol. Oceanogr.*, *53*(1), 212–224, doi:10.4319/lo.2008.53.1.0212.

Fasham, M. J. R., H. Ducklow, and S. M. McKelvie (1990), A nitrogen-based model of plankton dynamics in the ocean mixed layer, *J. Mar. Res.*, *48*, 591–639.

Francois, R., S. Honjo, R. Krishfield, and S. Manganini (2001), Factors controlling the flux of organic carbon to the bathypelagic zone of the ocean, *Global Biogeochem. Cycles*, *16*(4), 1087, doi:10.1029/2001GB001722.

Klaas, C., and D. Archer (2002), Association of sinking organic matter with various types of mineral ballast in the deep sea: Implications for the rain ratio, *Global Biogeochem. Cycles*, *16*(4), 1116, doi:10.1029/2001GB001765.

Kriest, I., and G. T. Evans (1999), Representing phytoplankton aggregates in biogeochemical models, *Deep Sea Res., Part I*, *46*(11), 1841–1859, doi:10.1016/S0967-0637(99)00032-1.

Kwon, E. Y., F. Primeau, and J. L. Sarmiento (2009), The impact of remineralization depth on the air-sea carbon balance, *Nat. Geosci.*, *2*(9), 630–635, doi:10.1038/ngeo612.

Lampitt, R. S., K. F. Wishner, C. M. Turley, and M. V. Angel (1993), Marine snow studies in the Northeast Atlantic Ocean: Distribution, composition and role as a food source for migrating plankton, *Mar. Biol.*, *116*(4), 689–702, doi:10.1007/BF00355486.

Lampitt, R. S., B. Boorman, L. Brown, M. Lucas, I. Salter, R. Sanders, K. Saw, S. Seeyave, S. J. Thomalla, and R. Turnewitsch (2008), Particle export from the euphotic zone: Estimates using a novel drifting sediment trap, ^{234}Th and new production, *Deep Sea Res., Part I*, *55*(11), 1484–1502, doi:10.1016/j.dsr.2008.07.002.

Lampitt, R. S., I. Salter, and D. Johns (2009), Radiolaria: Major exporters of organic carbon to the deep ocean, *Global Biogeochem. Cycles*, *23*, GB1010, doi:10.1029/2008GB003221.

Lampitt, R. S., I. Salter, B. A. de Cuevas, S. Hartman, K. E. Larkin, and C. A. Pebody (2010), Long-term variability of downward particle flux in the deep northeast Atlantic: Causes and trends, *Deep Sea Res., Part II*, *57*(15), 1346–1361, doi:10.1016/j.dsr2.2010.01.011.

Lee, C., M. L. Peterson, S. G. Wakeham, R. A. Armstrong, J. K. Cochran, J. C. Miquel, S. W. Fowler, D. Hirschberg, A. Beck, and J. Xue (2009), Particulate organic matter and ballast fluxes measured using time-series and settling velocity sediment traps in the northwestern Mediterranean Sea, *Deep Sea Res., Part II*, *56*(18), 1420–1436, doi:10.1016/j.dsr2.2008.11.029.

Lundsgaard, C. (1995), Use of a high viscosity medium in studies of aggregates, in *Sediment Trap Studies in the Nordic Countries 3. Proceeding of the Symposium on Seasonal Dynamics of Planktonic Ecosystems and Sedimentation in Coastal Nordic Waters*, edited by S. Floderus et al., pp. 141–152, Finn. Environ. Agency, Helsing, Denmark.

Martin, J. H., G. A. Knauer, D. M. Karl, and W. W. Broenkow (1987), VERTEX: Carbon cycling in the northeast Pacific, *Deep Sea Res., Part A*, *34*(2), 267–285, doi:10.1016/0198-0149(87)90086-0.

Martin, P., J. T. Allen, M. J. Cooper, D. G. Johns, R. S. Lampitt, R. Sanders, and D. A. H. Teagle (2010), Sedimentation of acantharian cysts in the Iceland Basin: Strontium as a ballast for deep ocean particle flux, and implications for acantharian reproductive strategies, *Limnol. Oceanogr.*, *55*(2), 604–614, doi:10.4319/lo.2009.55.2.0604.

McCave, I. N. (1975), Vertical flux of particles in the ocean, *Deep Sea Res. Oceanogr. Abstr.*, *22*(7), 491–502, doi:10.1016/0011-7471(75)90022-4.

Mullin, M. M. (1965), Size fractionation of particulate organic carbon in the surface waters of the western Indian Ocean, *Limnol. Oceanogr.*, *10*(3), 459–462, doi:10.4319/lo.1965.10.3.0459.

Nowald, N., G. Fischer, V. Ratmeyer, M. Iversen, C. Reuter, and G. Wefer (2009), In-situ sinking speed measurements of marine snow aggregates acquired with a settling chamber mounted to the Cherokee ROV, in *Oceans 2009-Europe*, pp. 1–6, Inst. of Electr. and Electr. Eng., Bremen, Germany, doi:10.1109/oceanse.2009.5278186.

Passow, U. (2004), Switching perspectives: Do mineral fluxes determine particulate organic carbon fluxes or vice versa?, *Geochem. Geophys. Geosyst.*, *5*, Q04002, doi:10.1029/2003GC000670.

Passow, U., and C. L. De La Rocha (2006), Accumulation of mineral ballast on organic aggregates, *Global Biogeochem. Cycles*, *20*, GB1013, doi:10.1029/2005GB002579.

Passow, U., R. F. Shipe, A. Murray, D. K. Pak, M. A. Brzezinski, and A. L. Alldredge (2001), The origin of transparent exopolymer particles (TEP) and their role in the sedimentation of particulate matter, *Cont. Shelf Res.*, *21*(4), 327–346, doi:10.1016/S0278-4343(00)00101-1.

Peterson, M., P. J. Hernes, D. S. Thoreson, J. I. Hedges, C. Lee, and S. G. Wakeham (1993), Field evaluation of a valved sediment trap, *Limnol. Oceanogr.*, *38*(8), 1741–1761, doi:10.4319/lo.1993.38.8.1741.

Peterson, M., S. G. Wakeham, C. Lee, M. A. Askea, and J. C. Miquel (2005), Novel techniques for collection of sinking particles in the ocean and determining their settling rates, *Limnol. Oceanogr. Methods*, *3*, 520–532, doi:10.4319/lom.2005.3.520.

Poulton, A. J., R. Sanders, P. M. Holligan, M. C. Stinchcombe, T. R. Adey, L. Brown, and K. Chamberlain (2006), Phytoplankton mineralization in the tropical and subtropical Atlantic Ocean, *Global Biogeochem. Cycles*, *20*, GB4002, doi:10.1029/2006GB002712.

Robinson, C., et al. (2010), Mesopelagic zone ecology and biogeochemistry: A synthesis, *Deep Sea Res., Part II*, *57*(16), 1504–1518, doi:10.1016/j.dsr2.2010.02.018.

Sanders, R., P. Morris, A. J. Poulton, M. C. Stinchcombe, A. Charalampopoulou, M. I. Lucas, and S. J. Thomalla (2010), Does a ballast effect occur in the surface ocean? *Geophys. Res. Lett.*, *37*, L08602, doi:10.1029/2010GL042574.

Sigman, D. M., and E. A. Boyle (2000), Glacial/interglacial variations in atmospheric carbon dioxide, *Nature*, *407*(6806), 859–869, doi:10.1038/35038000.

Steinhoff, T., T. Friedrich, S. E. Hartman, A. Oschlies, D. W. R. Wallace, and A. Kortzinger (2010), Estimating mixed layer nitrate in the North Atlantic Ocean, *Biogeosciences*, *7*(3), 795–807, doi:10.5194/bg-7-795-2010.

Thomalla, S. J., A. J. Poulton, R. Sanders, R. Turnewitsch, P. M. Holligan, and M. I. Lucas (2008), Variable export fluxes and efficiencies for calcite, opal, and organic carbon in the Atlantic Ocean: A ballast effect in action?, *Global Biogeochem. Cycles*, *22*, GB1010, doi:10.1029/2007GB002982.

Turner, J. T. (2002), Zooplankton fecal pellets, marine snow and sinking phytoplankton blooms, *Aquat. Microb. Ecol.*, *27*(1), 57–102, doi:10.3354/ame027057.

van der Loeff, M. R., et al. (2006), A review of present techniques and methodological advances in analyzing ^{234}Th in aquatic systems, *Mar. Chem.*, *100*(3–4), 190–212, doi:10.1016/j.marchem.2005.10.012.

Wakeham, S. G., C. Lee, M. L. Peterson, Z. Liu, J. Szlosek, I. F. Putnam, and J. Xue (2009), Organic biomarkers in the twilight zone–Time series and settling velocity sediment traps during MedFlux, *Deep Sea Res., Part II*, *56*(18), 1437–1453, doi:10.1016/j.dsr2.2008.11.030.

Wilson, S. E., D. K. Steinberg, and K. O. Buesseler (2008), Changes in fecal pellet characteristics with depth as indicators of zooplankton repackaging of particles in the mesopelagic zone of the subtropical and subarctic North Pacific Ocean, *Deep Sea Res., Part II*, *55*(14–15), 1636–1647, doi:10.1016/j.dsr2.2008.04.019.

E. P. Achterberg, C. Marsay, and J. S. Riley, School of Ocean and Earth Science, National Oceanography Centre Southampton, University of Southampton, Southampton SO14 3ZH, UK. (jennifer.riley@noc.soton.ac.uk)

F. A. C. Le Moigne, A. J. Poulton, and R. Sanders, National Oceanography Centre Southampton, Southampton SO14 3ZH, UK.